J|A|C|S
COMMUNICATIONS

Published on Web 02/16/2006

Backbone Conformational Constraints in a Microcrystalline U-^{15}N-Labeled Protein by 3D Dipolar-Shift Solid-State NMR Spectroscopy

W. Trent Franks, Benjamin J. Wylie, Sara A. Stellfox, and Chad M. Rienstra*

Department of Chemistry, Department of Biochemistry, and Center for Biophysics and Computational Biology, University of Illinois at Urbana−Champaign, 600 South Mathews Avenue, Urbana, Illinois 61801

Received December 6, 2005; E-mail: rienstra@scs.uiuc.edu

Structural studies of uniformly labeled proteins by magic-angle spinning (MAS) NMR have rapidly matured in recent years. Site-specific chemical shifts of several proteins have been assigned,[1,2] and structures have been determined from 2D or 3D data sets containing internuclear distance information.[3] Thus far, MAS NMR structures have a relatively low resolution in comparison to high-quality solution NMR or crystal structures, for two principal reasons: (1) the distance constraints extracted from multidimensional protein spectra are not yet as precise as those measured in small peptides and model compounds; (2) the number of constraints per residue is typically much less than that in solution NMR protein studies. These problems continue to be addressed by a variety of approaches, as recently reviewed.[4]

The direct determination of torsion angles by relative dipolar and/or chemical shift anisotropy (CSA) orientation measurements is a complementary approach for protein structure determination and refinement, which has enjoyed notable success in the studies of small peptides.[5−7] The magnitude of tensor interference effects observed in these experiments is roughly 1 kHz per 10° change in the torsion angle, at least an order of magnitude larger than the size of dipolar couplings utilized for long-range distance estimations. Thus, even measurements in large membrane proteins have been demonstrated with better than 10° precision.[8] However, the application of this strategy to multiply labeled proteins has been relatively limited,[9] and no study has yet reported such constraints for the majority of backbone torsion angles throughout a uniformly labeled solid protein.

Here we present such a study on the β1 immunoglobulin binding domain of protein G (GB1), for which we have recently reported complete ^{13}C and ^{15}N chemical shift assignments in a microcrystalline preparation.[2] GB1 presents an excellent system for development and systematic evaluation of high-resolution structure determination protocols for solid proteins, due to its mixed secondary structure, packing density, and thermal stability. Spectral resolution and sensitivity are exemplified by the 2D ^{15}N−^{15}N correlation spectrum (Figure 1), in which most peaks are uniquely resolved: 13 diagonal (N[i]−N[i]), 45 N[i]−N[$i\pm1$], and 9 N[i]−N[$i\pm2$] cross-peak pairs are assigned. The relative cross-peak intensities in this 2D spectrum can be used to estimate the N−N distances,[5] and the addition of a synchronous T-MREV H−N recoupling period[10] produces HN−HN dipolar line shapes in the third dimension.[5] Our experiments extend this idea to analyze a significantly larger range of geometries for HN[i]−HN[$i\pm1$] sites and include analysis of several HN[i]−HN[$i\pm2$] line shapes. The spectra altogether constrain 114 backbone torsion angles.

Quantitative cross-peak volumes were extracted and the HN T-MREV dephasing trajectories analyzed. The HN[i]−HN[i] spectra provide an important control for the simulation model, gauging the number of weakly coupled protons that must be included and constraining the dipolar scaling factor and differential relaxation rate.[6,10] The characteristic dipolar line shape for this geometry (Figure 2a) has a high-frequency component, arising from the sum of the H−N couplings, and a low-frequency component from the difference. When modeled accurately (details in Supporting Information), fits of the dipolar spectra reveal a pseudo-bond angle (θ) close to zero. For the 13 resolved diagonal sites in GB1, we found an average θ of 1.1 ± 1.0°; the deviations arise from approximations in modeling the effects of proton CSA as relaxation in the average Liouvillian model.[6,10] This systematic error is small compared to the random errors in the cross-correlated line shapes (Figure 2b−f). A full statistical analysis (Supporting Information) reveals better than ±5° (σ) precision for most sites, in very good agreement with a new 1.14 Å crystal structure also determined as part of this study. Observed line shapes fit to $\theta = \sim7$ to ~80° and are summarized by comparing θ_{NMR} versus to θ_{X-RAY} (Figure 3). Helical conformations have especially high precision since the N[i]−N[$i\pm1$] cross-peaks have very good sensitivity, and θ is ~15 to 20°, a region with strong orientation dependence; for example, N35-D36 (Figure 2c) has $\theta_{SSNMR} = 18.6 \pm 0.9°$ and $\theta_{X-RAY} = 17.5°$. Likewise β-strand conformations typically have $\theta = 150$ to 170° (by symmetry equivalent to 10 to 30°); for example, T55-E56 (Figure 2b) has $\theta_{SSNMR} = 11.8 \pm 1.7°$ and $\theta_{X-RAY} = 14.7°$. The majority of sites agree within the experimental SSNMR error (±2 σ). We

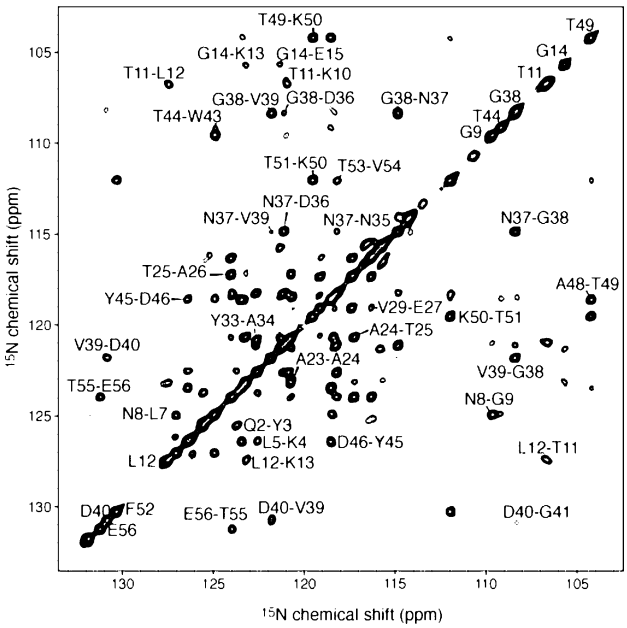

Figure 1. ^{15}N−^{15}N proton-driven spin-diffusion correlation spectrum of GB1 (the first 2D plane from the 3D {HN}−N−N experiment, 599.46 MHz ^{1}H frequency, 2 s mixing time). Time domains were digitized to 45.6 ms in t_1 and 61.44 ms in t_2, with a total measurement time of 12 h. Most N[i]−N[i+1] and several N[i]−N[i+2] correlations are resolved. Complete assignments are presented in the Supporting Information.

10.1021/ja058292x CCC: $33.50

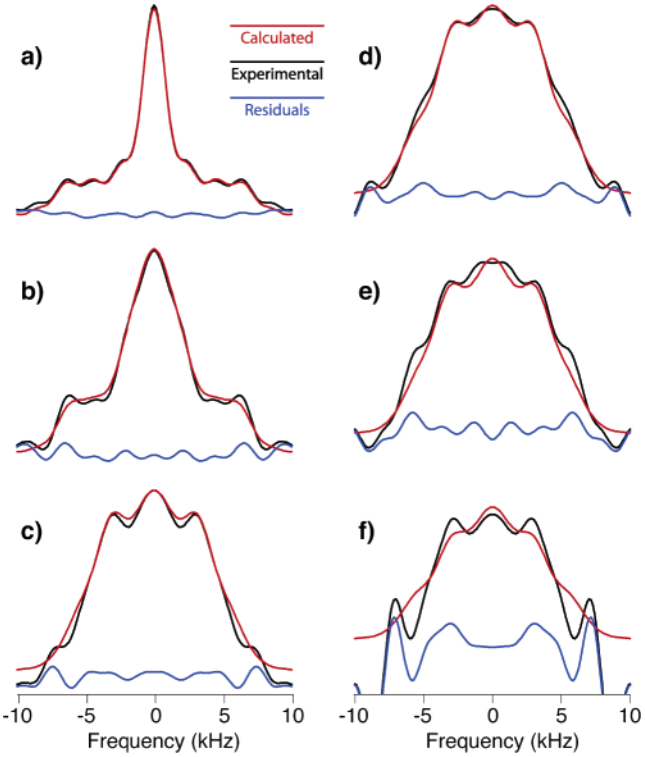

Figure 2. Amide−amide dipolar line shapes in GB1. Representative examples of (a) an autocorrelated peak (W43, $\theta = 0.4 \pm 0.9°$), (b) an α-helical pair (N35-D36, $\theta = 18.6 \pm 0.9°$), (c) a β-strand pair (D47-A48, $\theta = 48.8 \pm 3.4°$), (d) a coil (D36-N37, $\theta = 62.3 \pm 2.5°$), (e) a β-turn (T49-K50, $\theta = 49.0 \pm 6.9$), and (f) a N[i]−N[i+2] correlation (D36-G38, $\theta = 38.4 \pm 8.0°$).

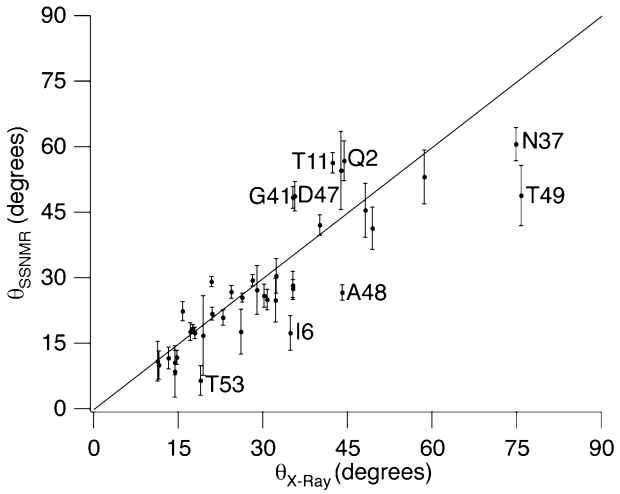

Figure 3. Comparison of pseudo-bond HN[i]−HN[i+1] angles determined by SSNMR and crystallography. Error bars for the SSNMR data are ±1 σ. The RMSD between the SSNMR and X-ray values is 8.9°. The largest disagreements are found in turns, due to statistically significant structural differences between the samples. Select outlying residues are labeled; the complete table of data is provided in the Supporting Information.

attribute the remaining variations in regular secondary structure elements to the inaccuracy of proton positions in the crystal structure, modeled with standard bond angles.

Turn geometries are especially important for defining overall protein folds and are poorly constrained by semiempirical methods, such as TALOS.[11] Our results are more precise than TALOS for these residues, and HN[i]−HN[$i\pm2$] line shapes offer additional constraints; for example, D36-G38 (Figure 2f) has $\theta_{SSNMR} = 38.4 \pm 8.0°$ and $\theta_{X-RAY} = 35.7°$. Not all of the turn geometries agree with the crystal structure (e.g., T11, G41, A48, T49). We attribute these discrepancies to real conformational differences between the SSNMR and X-ray samples since growing the single crystal required higher salt and lower pH than the SSNMR sample. We expect that refinement using pseudo-bond angles as direct structural constraints will improve the structure further.

The fact that such good overall agreement is observed in GB1 may be in part attributed to its high sensitivity and resolution. However, the generality of this approach is supported by previous work[12,13] in which improvements in proton-detected experiments of other proteins have been demonstrated. Higher magnetic fields, gradients, deuteration with amide back-exchange, and/or 3D experiments are known to enhance ^{1}H−^{15}N resolution and sensitivity. We reasonably expect that the combination of ^{1}H−^{15}N dipole vector experiments with these established techniques will facilitate high-resolution structure determination in a general way.

Acknowledgment. The authors thank the University of Illinois, American Chemical Society (Petroleum Research Fund), and National Science Foundation (MCB 0347824) for funding, and Drs. Yi Gui Gao and Scott Wilson (George L. Clark X-ray Facility) for technical assistance.

Supporting Information Available: Details of the data acquisition, processing and fitting procedures; a table of measured angles; comparison to TALOS results. This material is available free of charge via the Internet at http://pubs.acs.org.

References

(1) (a) Pauli, J.; Baldus, M.; van Rossum, B.; de Groot, H.; Oschkinat, H. *ChemBioChem* **2001**, *2*, 272−281. (b) Bockmann, A.; Lange, A.; Galinier, A.; Luca, S.; Giraud, N.; Juy, M.; Heise, H.; Montserret, R.; Penin, F.; Baldus, M. *J. Biomol. NMR* **2003**, *27*, 323−339. (c) Igumenova, T. I.; Wand, A. J.; McDermott, A. E. *J. Am. Chem. Soc.* **2004**, *126*, 5323−5331. (d) Marulanda, D.; Tasayco, M. L.; Cataldi, M.; Arriaran, V.; Polenova, T. *J. Phys. Chem. B* **2005**, *109*, 18135−18145.

(2) Franks, W. T.; Zhou, D. H.; Wylie, B. J.; Money, B. G.; Graesser, D. T.; Frericks, H. L.; Sahota, G.; Rienstra, C. M. *J. Am. Chem. Soc.* **2005**, *127*, 12291−12305.

(3) (a) Castellani, F.; van Rossum, B.; Diehl, A.; Schubert, M.; Rehbein, K.; Oschkinat, H. *Nature* **2002**, *420*, 98−102. (b) Castellani, F.; van Rossum, B. J.; Diehl, A.; Rehbein, K.; Oschkinat, H. *Biochemistry* **2003**, *42*, 11476−11483. (c) Zech, S. G.; Wand, A. J.; McDermott, A. E. *J. Am. Chem. Soc.* **2005**, *127*, 8618−8626. (d) Lange, A.; Becker, S.; Seidel, K.; Giller, K.; Pongs, O.; Baldus, M. *Angew. Chem., Int. Ed.* **2005**, *44*, 2089−2092.

(4) McDermott, A. E. *Curr. Opin. Struct. Biol.* **2004**, *14*, 554−561.

(5) Reif, B.; Hohwy, M.; Jaroniec, C. P.; Rienstra, C. M.; Griffin, R. G. *J. Magn. Reson.* **2000**, *145*, 132−141.

(6) Rienstra, C. M.; Hohwy, M.; Mueller, L. J.; Jaroniec, C. P.; Reif, B.; Griffin, R. G. *J. Am. Chem. Soc.* **2002**, *124*, 11908−11922.

(7) Rienstra, C. M.; Tucker-Kellogg, L.; Jaroniec, C. P.; Hohwy, M.; Reif, B.; McMahon, M. T.; Tidor, B.; Lozano-Perez, T.; Griffin, R. G. *Proc Natl. Acad. Sci. U.S.A.* **2002**, *99*, 10260−10265.

(8) (a) Feng, X.; Verdegem, P. J. E.; Lee, Y. K.; Sandström, D.; Edén, M.; Bovee-Geurts, P.; de Grip, W. J.; Lugtenburg, J.; de Groot, H. J. M.; Levitt, M. H. *J. Am. Chem. Soc.* **1997**, *119*, 6853−6857. (b) Lansing, J. C.; Hohwy, M.; Jaroniec, C. P.; Creemers, A. F. L.; Lugtenburg, J.; Herzfeld, J.; Griffin, R. G. *Biochemistry* **2002**, *41*, 431−438.

(9) (a) Hong, M. *J. Magn. Reson.* **1999**, *139*, 389−401. (b) Ladizhansky, V.; Jaroniec, C. P.; Diehl, A.; Oschkinat, H.; Griffin, R. G. *J. Am. Chem. Soc.* **2003**, *125*, 6827−6833.

(10) Hohwy, M.; Jaroniec, C. P.; Reif, B.; Rienstra, C. M.; Griffin, R. G. *J. Am. Chem. Soc.* **2000**, *122*, 3218−3219.

(11) Cornilescu, G.; Delaglio, F.; Bax, A. *J. Biomol. NMR* **1999**, *13*, 289−302.

(12) Paulson, E. K.; Morcombe, C. R.; Gaponenko, V.; Dancheck, B.; Byrd, R. A.; Zilm, K. W. *J. Am. Chem. Soc.* **2003**, *125*, 15831−15836.

(13) Chevelkov, V.; van Rossum, B. J.; Castellani, F.; Rehbein, K.; Diehl, A.; Hohwy, M.; Steuernagel, S.; Engelke, F.; Oschkinat, H.; Reif, B. *J. Am. Chem. Soc.* **2003**, *125*, 7788−7789.

JA058292X